International Journal of Impact Engineering 181 (2023) 104757

Contents lists available at ScienceDirect

International Journal of Impact Engineering

journal homepage: www.elsevier.com/locate/ijimpeng

Impact response of advance combat helmet pad systems

M. Rodriguez-Millan [a,*], I. Rubio [a], F.J. Burpo [b], A. Olmedo [c], J.A. Loya [d], K.K. Parker [b,e], M. H Miguélez [a]

[a] Department of Mechanical Engineering, University Carlos III of Madrid, Avda. de la Universidad 30, 28911 Leganés, Madrid, Spain
[b] Department of Chemistry and Life Science, United States Military Academy, West Point, 10996, N.Y., United States
[c] FECSA Company Calle de Acacias 3, 28703, San Sebastián de los Reyes, Madrid, Spain
[d] Department of Continuum Mechanics and Structural Analysis, University Carlos III of Madrid, Avda. de la Universidad 30, 28911 Leganés, Madrid, Spain
[e] Disease Biophysics Group, Wyss Institute for Biologically Inspired Engineering, John A. Paulson School of Engineering and Applied Sciences, Harvard University, 29 Oxford Street, Pierce Hall 318, Cambridge, MA 02138, United States of America

ARTICLE INFO

Keywords:
Hybrid III
Impact
Ballistic
TBI
Lower neck injury
FMJ

ABSTRACT

Combat helmets are designed to protect against ballistic threats and fragments of explosive devices. There are numerous types of helmet comfort foams available. However, pad systems have not been evaluated in combat helmets to understand to what extent they mitigate head accelerations. In this work, different pad systems are studied to analyze the ballistic performance of combat helmets using a Hybrid III dummy equipped with longitudinal accelerometers at the head and a neck simulator. The tests are conducted with 9 mm Full Metal Jacket (FMJ) projectiles according to the performance requirements III-A of the NIJ 0106.01 standard. This experimental methodology allows the evaluation of brain and neck injuries. The thicker bicomponent polyurethane foams and the honeycomb configuration provided the best results in terms of mitigating brain damage due to accelerations applying different criteria (PLA, WSTC, HIC). However, it was concluded that there is no cervical injury or cranial fracture risk for any of the cases studied.

1. Introduction

Mild traumatic brain (mTBI) and neck injuries have a high social and economic cost. Still, they are challenging to assess and quantify compared to injuries to other body parts. In industrialized countries, traumatic injuries are the leading cause of fatalities under 45 years old. Traumatic brain injury is a complex medical problem to study because of the disease's wide range of spatial and temporal scales [1]. The most common mechanisms causing brain and neck injuries are traffic accidents (36.3%), followed by falls (35.2%), direct impacts (22.3%), and being run over by a vehicle (5.2%) [2]. During military armed conflict, the risk of brain damage in civilians and the military increases. During the United States' war in Afghanistan (10-07-2001 – 08-31-2021), approximately 9–28% of U.S. military service members who participated suffered a traumatic brain injury (TBI) [3,4]. Primary traumatic brain injury is mainly caused by high-energy mechanical loads such as bullet penetration or violent impact [5]. The design of modern combat helmets is the most effective device to reduce brain injury and is a priority for leading governments, military industrialists, and researchers.

Literature focused on the analysis of the ballistic behavior of the helmet and mainly deals with the blunt helmet measured with a normalized human head surrogate with Roma clay witness and the ballistic limit velocity of the helmet, V_{50} (the velocity at which the probability of perforation is 50 percent) [6–12].

However, there has been limited research on the biomechanical response to ballistic impact based on accelerations and pressures affecting the brain and deformations produced in the skull both experimentally [13,14] and numerically [15–19]. Some authors have performed ballistic impact tests on combat helmets using head simulants instrumented with accelerometers and pressure sensors [20–22]. Highlighting the work by Begonia et al. [23], where they analyzed the impact difference between the results on the impact on ACH helmet mounted on ATDs and PMHS (Post Mortem Human Subject), obtaining differences of 18% in linear acceleration peaks, so, due to the physiological and morphological differences between the simulant and the PMHS, it can be considered acceptable. Thus, it can be assumed that the ATD dummy reproduces, in terms of acceleration, the behavior of a real human head with an acceptable correlation.

* Corresponding author.
E-mail address: mrmillan@ing.uc3m.es (M. Rodriguez-Millan).

https://doi.org/10.1016/j.ijimpeng.2023.104757
Received 24 May 2023; Received in revised form 24 July 2023; Accepted 12 August 2023
Available online 19 August 2023

Most studies have focused on evaluating the performance of the combat helmet shell; however, the influence of the pad system may have a relevant role in minimizing TBI. Tse et al. [24] numerically analyzed through finite element modeling the TBI mitigation performance of two types of interior energy absorbing systems, OA foam and strap netting, considering different impact locations. This study also analyzed the biomechanical response to impacts in over-pad and pad-free zones.

Brain injury occurs significantly on impact of a projectile in the frontal location of the combat helmet [10–12,25] due to head-to-helmet clearance being smaller than in other directions. In addition, some authors in different areas, such as sports or industrial safety, have focused their studies considering frontal impacts, which induce greater accelerations than in other locations [26–32]. Recently, the authors conducted an experimental and numerical study of FMJ 9 mm projectile impacts on aramid combat helmets at different locations [33]. The results showed that frontal and rear impacts were the most critical. Therefore, this work has chosen to compare the ballistic performance of different foams through frontal impacts based on the results of the author's previous work [33] and previous studies by other authors such as Tse et al. [24] where similar conclusions were reached.

Efforts to improve the ballistic performance of the combat helmet have focused on reducing brain damage. However, neck injuries could potentially be caused by the combination of forces and moments due to the projectile's impact. Neck injuries are generally related to the helmet weight; there is a low probability of neck injury when a heavier helmet is used due to lower neck forces and, therefore, more significant damage mitigation [34]. The risk of neck injury is low because the velocity components will be lower with a heavier helmet [35].

The first neck damage criteria were elaborated through sled tests with dummies, volunteers, and cadavers, establishing maximum tolerance limits for each type of load that could occur: axial tension and compression and bending and extension moments [36–38]. However, this formulation does not consider the combined effects of moments and axial loads. Later, in 1984, Prasad and Daniel [39] proposed a combined criterion of tension loads and extension (backward) moments based on experimental studies on porcine subjects.

The criterion was then extended by considering the combination of the four types of neck loading modes based on the studies of Prasad and Daniel [39]. The resulting criteria are denoted N_{ij}, where "ij" represents indices for the four injury mechanisms, namely N_{TE}, N_{TF}, N_{CE}, and N_{CF}. The first index represents axial loading (tensile or compressive), and the second index represents sagittal plane bending moment (flexion or extension). A Hybrid III 50th percentile dummy presents critical values of 3600 N for tension/compression axial load and 410 Nm and 125 Nm for flexion and extension moment, respectively. This criterion is developed for the upper neck load cell that records forces and moments in the three x,y, and z directions. Consequently, with the proposed formulation N_{ij}, only the three measurements associated with motion in the sagittal plane are used: axial load (F_z), shear load (F_x), flexion/extension moment (M_y) [40,41]. The criterion for neck damage is therefore formulated as follows, Eq. (1).

$$N_{ij} = \frac{F_z}{F_{int}} + \frac{M_y}{M_{int}} \tag{1}$$

where F_z is the axial load, F_{int} is the maximum tolerance value of load, M_y is flexion/extension moment and M_{int} is the maximum tolerance value for moment in the sagittal plane.

Lower neck injury (LNI) refers to injuries that occur in the lower cervical spine, specifically the vertebrae C3/C5 to C7 (depending on the author/work). Yoganandan et al. [42,43] later developed a neck injury criterion based on forces and moments at the base of the neck referred to as lower neck injury criteria. In their work, Yoganandan et al. [42,43] later developed a neck injury criterion based on forces and moments at the base of the neck, referred to as the lower neck injury criteria. In their work, Yoganandan et al. [42] experimentally characterized the mechanical and geometric properties of the cervical ligaments to study the biomechanical behavior of the human cervical spine. In 2017, Yoganandan et al. [44] performed tests on human cadavers to characterize and develop the failure criterion in both men and women subjected to rear impact in moving vehicles. Subsequently, in 2020, Yoganandan et al. [45] derived lower neck injury probability curves from testing rear impact situations for dummy Hybrid III and Thor. The critical values were obtained from the force and moment risk curves corresponding to a 90% probability level. However, Begonia [46] compared the difference between the ATD necks (hybrid III and EuroSid-using the NOCSAE normalized head) by analyzing the extension and deflection under rear and frontal impact.

There is a lack of a complete analysis of ballistic impact on combat helmets, including different criteria such as helmet deformation in the literature, brain damage through acceleration analysis, and neck damage criteria. In the same way, it has been observed in the literature that the energy absorption internal system is not analyzed and that the studies are mainly focused on the integrity of the combat helmet.

The main contribution involves evaluating and comparing the ballistic performance of four-pad systems designed for combat helmets. In this work, we examine the potential injury caused by the ballistic impact based on two independent criteria: the brain injury criterion, taking into account the accelerations measured in the dummy Hybrid III head, and the injury at the lower neck reaction forces and moments.

The ballistic tests have been carried out using 9 mm Full Metal Jacket (FMJ) projectiles and following the III-A performance requirements set by the United States National Institute of Justice [47]. Combat helmets with different pad systems are fitted on a Hybrid III dummy to evaluate longitudinal accelerations, neck forces, and moments. The pad systems used in this work have different areal densities, thicknesses, and designs. The features of the foam systems can lead to variations in the data recorded in accelerations and forces, and moments in the neck. Therefore, its evaluation is important to advance knowledge about minimizing brain and neck injuries in combat helmets. Additionally, postmortem helmet backface deformation for each configuration is evaluated using a 3D scanner.

For this purpose, the combat helmet, pad systems, and experimental setup are presented in Section 2. An analysis of the brain and neck injury to evaluate the helmet and the different pad systems is also carried out. Section 3 presents the results collected from the Hybrid III dummy head accelerometers and neck load cell. With these experimental data, Section 4 performs a brain injury analysis using the peak longitudinal acceleration criterion (PLA) and the Head Injury Criterion (HIC). Using data from the neck load cell, we assess the efficacy of the foams by employing the most recent low neck injury criterion from the literature. The conclusions of our evaluation are presented in the final section.

2. Experimental setup

2.1. Materials

2.1.1. Combat helmet

The Advanced Combat Helmet (ACH) helmet, commonly researched in the literature [7,11,12,48,49], developed with ultra-high molecular weight polyethylene (UHMWPE) with an areal density of 7 kg/m^2 (Manufactured by FECSA, Spain), is used to support the different pads analyzed in this work. The maximum dimensions of the helmet are 276 mm × 252 mm × 165 mm, referring to the front to rear, side to side, and height. The helmet thickness is approximately 8 mm. For this work, there is no different size of helmet shells. Still, it is achieved by coupling foams of different thicknesses, thus obtaining a more versatile and economical single helmet to manufacture.

2.1.2. Foam pad system

- Pad system I (S-I M and S-I G)

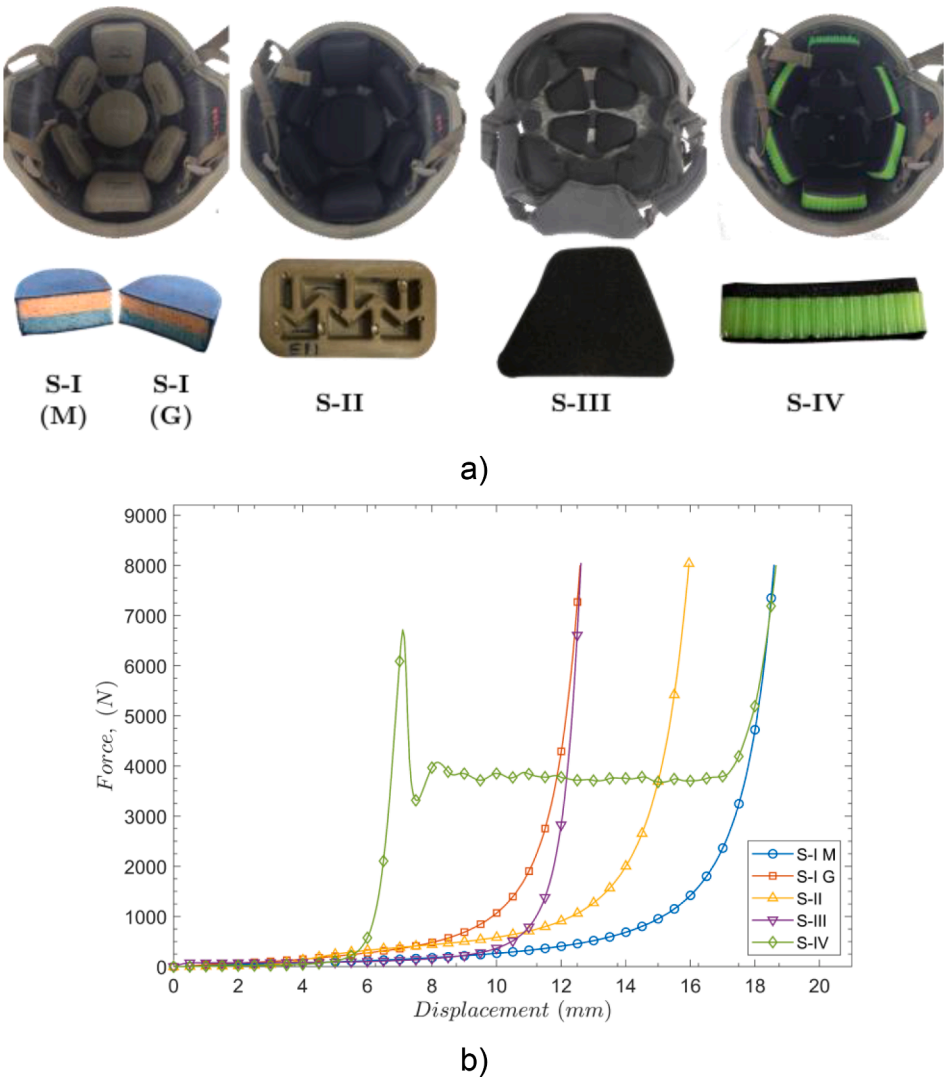

Fig. 1. Different foam pads systems. A) Disposition and visual shape description of foam pads. B) Quasi-static compression testing of different pad systems.

Table 1
Properties of pad systems for front side.

	S-I M	S-I G	S-II	S-III	S-IV
$t\ (mm)$	21	14	21	15	21
$\rho_{areal}\ (kg/m^2)$	2.80	2.33	3.17	1.29	1.35
$W_{abs}(J)$	13.58	10.60	13.41	6.30	49.76
$m\ (g)$	23.1	19.3	25	22.5	6.8
$SEA\ (J/g)$	0.58	0.54	0.53	0.28	7.31

The internal pad system I (denoted as S-I) is commonly used in the defense industry. The pad consists of a two-component, rigid and soft portion of the foam, having a density of 89.6 kg/m^3 for the rigid portion and 86.9 kg/m^3 for the softer portion. The foams are inside a waterproof polymeric wrapper and a cloth bag. This configuration comprises seven pads (one circular pad at the top of the head, one rectangular pad at the front and one at the back, and four oval side pads on each side of the head), as is shown in Fig. 1. In this configuration, two sizes are used: size G (denoted as *S-I G*), thickness, $t = 14$ *mm,* and M (*S-I M*), $t = 21$ *mm*. For the frontal pad, the areal densities are *2.33 kg/m^2* for size G and *2.80 kg/m^2* for size M.

- Pad system II (S-II)

The second system is based on a general-purpose sports pad. The foam system is composed of a soft polymer (integrated comfort liner) and a stiffer polymer with an auxetic deformation response. The system consists of 7 foam pads: one circular pad at the top, two square pads for the front and rear, and four rectangular pads for the sides. The thickness is *21 mm,* and the areal density is *3.17 kg/m^2*.

- Pad system III (S-III)

The third system is made of a single flexible material. The system consists of six components with three different geometries to adapt to the shape of the shell's interior. The thickness is *15 mm,* and the areal density is *1.29 kg/m^2*.

- Pad system IV (S-IV)

System IV comprises a sandwich configuration that combines outer comfort layers and circular geometry with a honeycomb panel core. The thickness is *21 mm,* and the areal density is *1.35 kg/m^2*.

A Universal Testing Machine Instron 3366 performs quasi-static compressive loading to obtain the energy absorption capacity (W_{abs}), Table 1. Energy absorption is defined as the area under a force-extension curve. In addition, the specific energy absorption (SEA) is also obtained as energy absorption per unit mass.

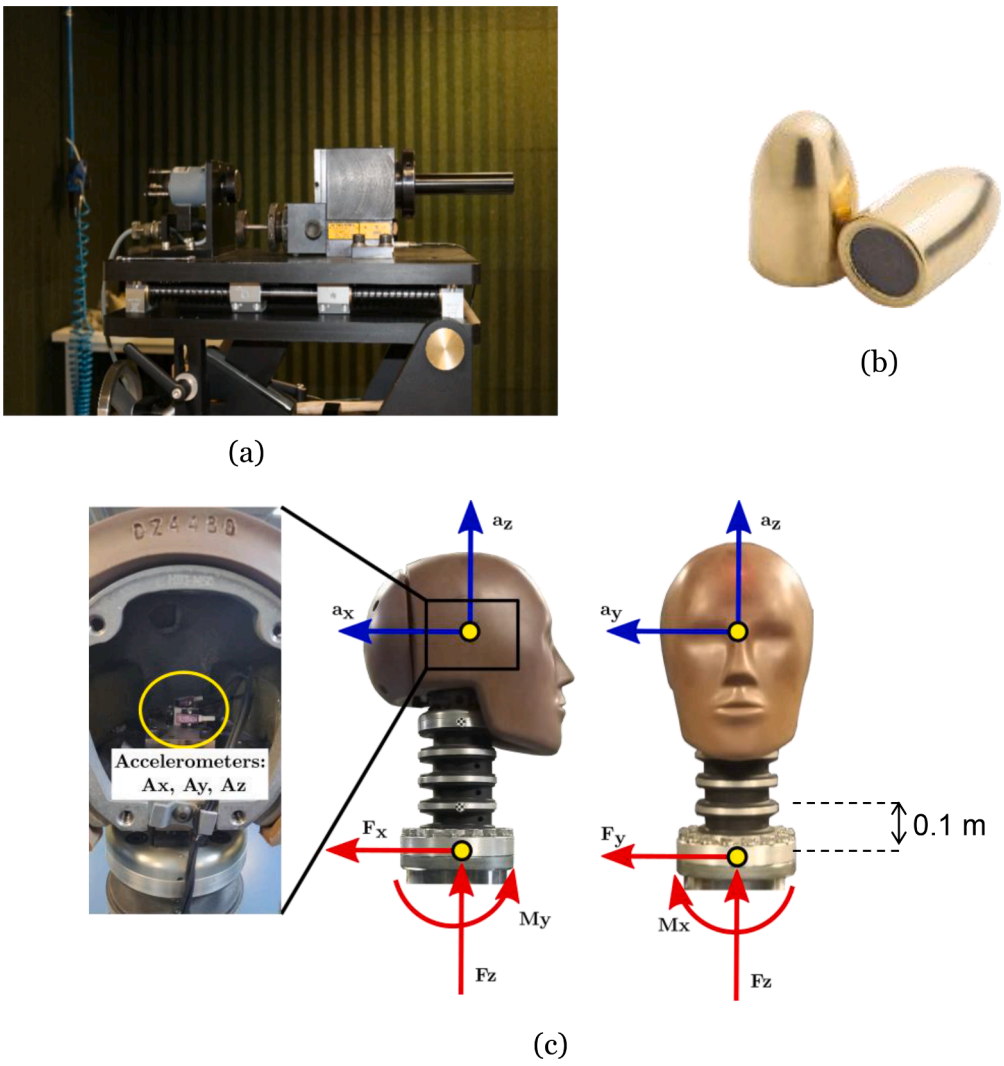

Fig. 2. Experimental setup. (a) Pneumatic cannon, (b) 8 g FMJ and (c) the Hybrid III 50th percentile ATD head and neck.

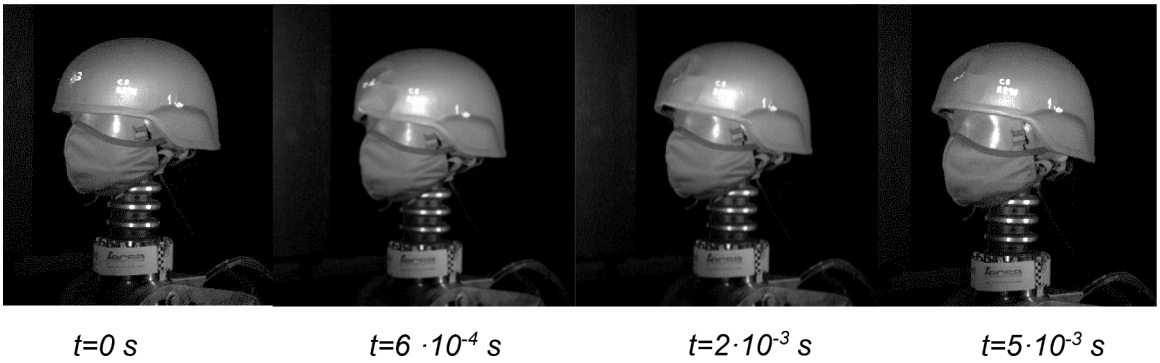

Fig. 3. A 425 m/s FMJ projectile impact sequence captured by a high-speed camera on a UHMWPE ACH combat helmet with bicomponent foams (Manufactured by FECSA, Spain).

All pad systems have a hyperelastic behavior except S-IV, which reaches its maximum force, and then its resistance drops by 40% due to its tubular honeycomb cell composition, Fig. 1. This behavior leads to the S-IV foam with the highest energy absorption capacity. The foams with the next higher energy absorption capacity are the 21 mm thick bicomponent foam (S-I M) and the 21 mm thick closed-cell foam (S-II). The foam with the lowest energy absorption is the S-III pad system due to its lower thickness of 15 mm. S-III has a lower energy absorption capacity than the 14 mm thick bicomponent foam (S-I G). Regarding the SEA, there is no direct relationship between thickness and SEA since the 14 mm thick S-IG has a higher SEA than the 21 mm thick S-II foam.

2.2. Human head surrogate

This work uses a hybrid-III anthropomorphic test dummy (ATD) head and neck assembly. The Hybrid III is instrumented to measure the

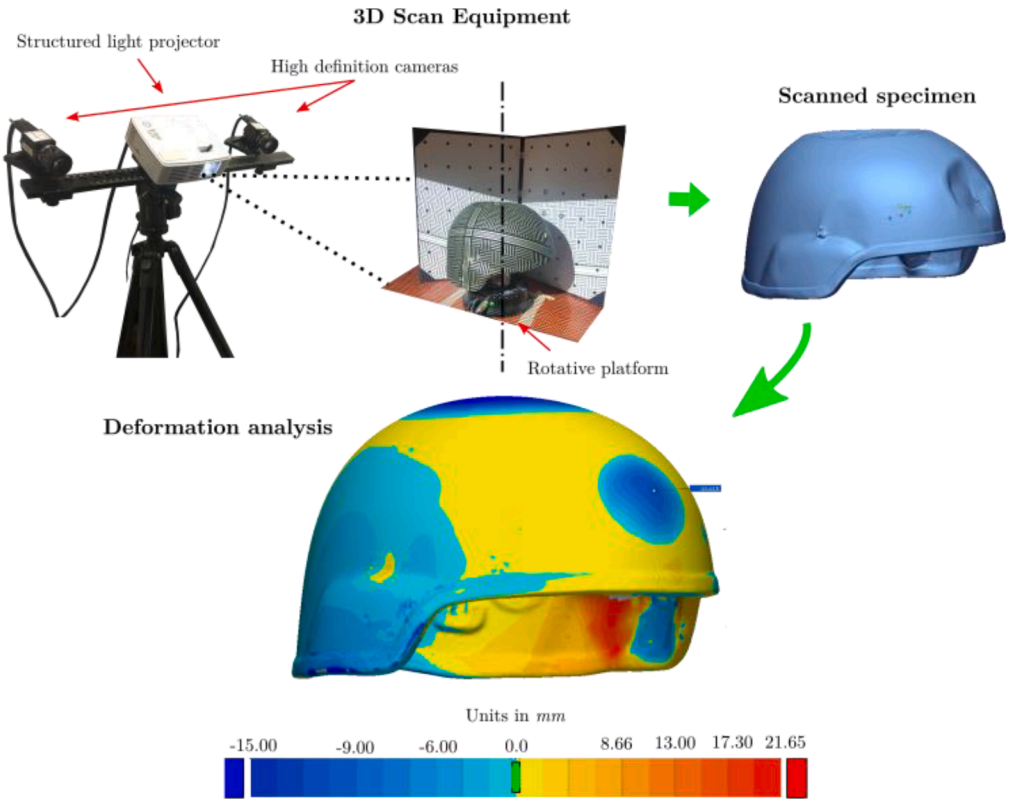

Fig. 4. A 3D scanner is used to measure helmets' permanent deformation. The combat helmets are scanned using two cameras and a light projector, and GeoMagic ControlX software is used to create a map of the helmet's deformations (in mm).

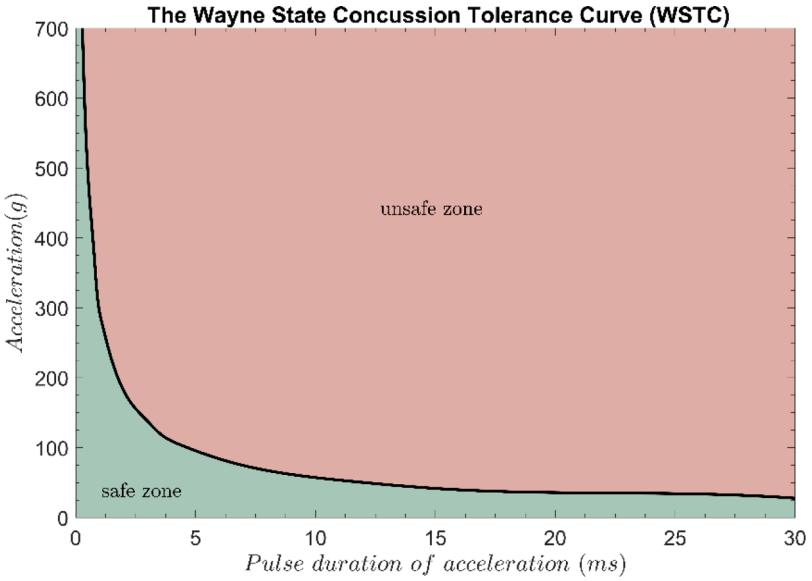

Fig. 5. The Wayne State Concussion Tolerance Curve (WSTC) is used to examine the relationship between Peak Linear Acceleration (PLA) and pulse duration. Safe zone in green and the unsafe zone in red [52,53].

three linear accelerations (a_x, a_y, a_z) at the head center of gravity, six lower neck forces (F_x, F_y, F_z), and moments (M_x, M_y, M_z). The accelerometers used are T.E. Connectivity 64C-2000-360T. The accelerometers are mounted on a bracket that ensures their position at the head's center of gravity. This support is fixed to the metallic inner skull. Fig. 2c shows a detailed view of the accelerometers inside the head. All data are collected at *50,000 Hz* by a DEWETRON DEWE-800 system, filtered according to SAE J211 [50]. SAE J211 filter consists of a *1650 Hz* lowpass (4-channel Butterworth) filter that removes high-frequency vibrations from the impact to the headform. The moments measured by this supracondylar load cell are translated inferiorly to the occipital condyles by multiplying respective *x-axis* shear forces by the appropriate *0.1 m* moment arm, Fig. 2c.

$$M_{yo} = M_y + 0.1 \cdot F_x \tag{2}$$

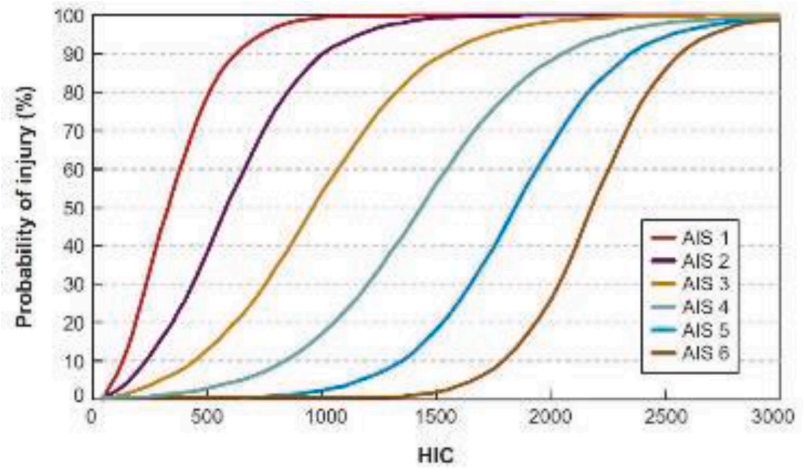

Fig. 6. Head injury risk curves, according to the AIS scale, based on the Head Injury Criteria (HIC). Adopted from Hayes et al. [56].

Table 2
Explanation of severity code [56].

AIS code	Severity code	Fatality rate (range%)
1	Minor	0.0
2	Moderate	0.1 – 0.4
3	Serious	0.8 – 2.1
4	Severe	7.9 – 10.6
5	Critical	53.1 – 58.4
6	Maximum	Untreatable

2.3. Ballistic impact devices

Experimental tests are conducted with a cannon gas gun with a rifled barrel, Fig. 2a. The helmet foam performance is evaluated through ballistic impact from the ammunition 9 × 19 *mm* Luger (a full-metal jacket and soft-lead core) with a mass of *8 g* at *430 m/s* according to the performance requirements III-A of NIJ 0106.01 standard [47], Fig. 2b.

The initial impact velocity and dummy's movement are recorded with two high-speed cameras, Photron FASTCAM SA-Z type 2100K-M-32 GB, mounted on tripods. Based on early testing, the selected frame rate (28,000 frames per second, fps) and the resolution (1024 × 744 pixels) are chosen, to allow a proper focus of the images. High-intensity lighting equipment is used to obtain good image quality. A high-intensity and low-flicker spotlight ARRI brand model with an 1800 W HMI lamp is used for getting a good image quality. The impact sequence is illustrated in Fig. 3.

2.4. Permanent backface deformation (PBFD)

Postmortem deformations are measured using 3D scan equipment (model H.P. 3D Structured Light Scanner Pro-S3 with 60–500 mm^3 scanning volume). The scanner allows the comparing of post-impacted deformations with a reference helmet without damage. A structured light projector, ACER model K132, develops a black/white line pattern beam and RGB light on the object (structured light). Two H.P. high-definition cameras capture the screenings for the stereoscopic image. Helmets are positioned on an automatic 360 ° rotating platform to capture the complete model and different positions due to their complex curvature.

The final impact geometry is exported to GeoMagic ControlX. It is an inverse engineering software that compares postmortem specimens with undeformed shapes (scanned or CAD models). It obtains the plate deflection depending on the type of projectile and impact velocity. A graphical scheme of the scanning process is illustrated in Fig. 4.

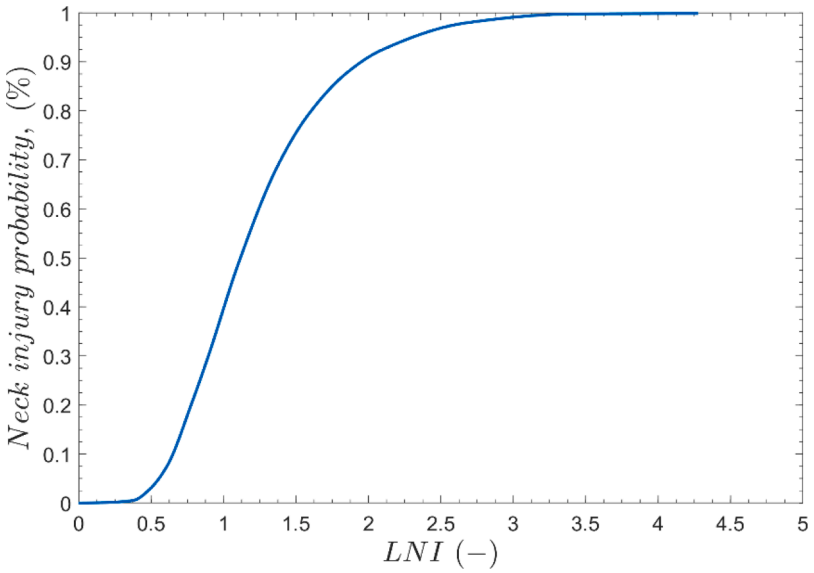

Fig. 7. Relationship between Lower Neck Injury (LNI) and injury probability. Adapted from Yoganandan et al. [45].

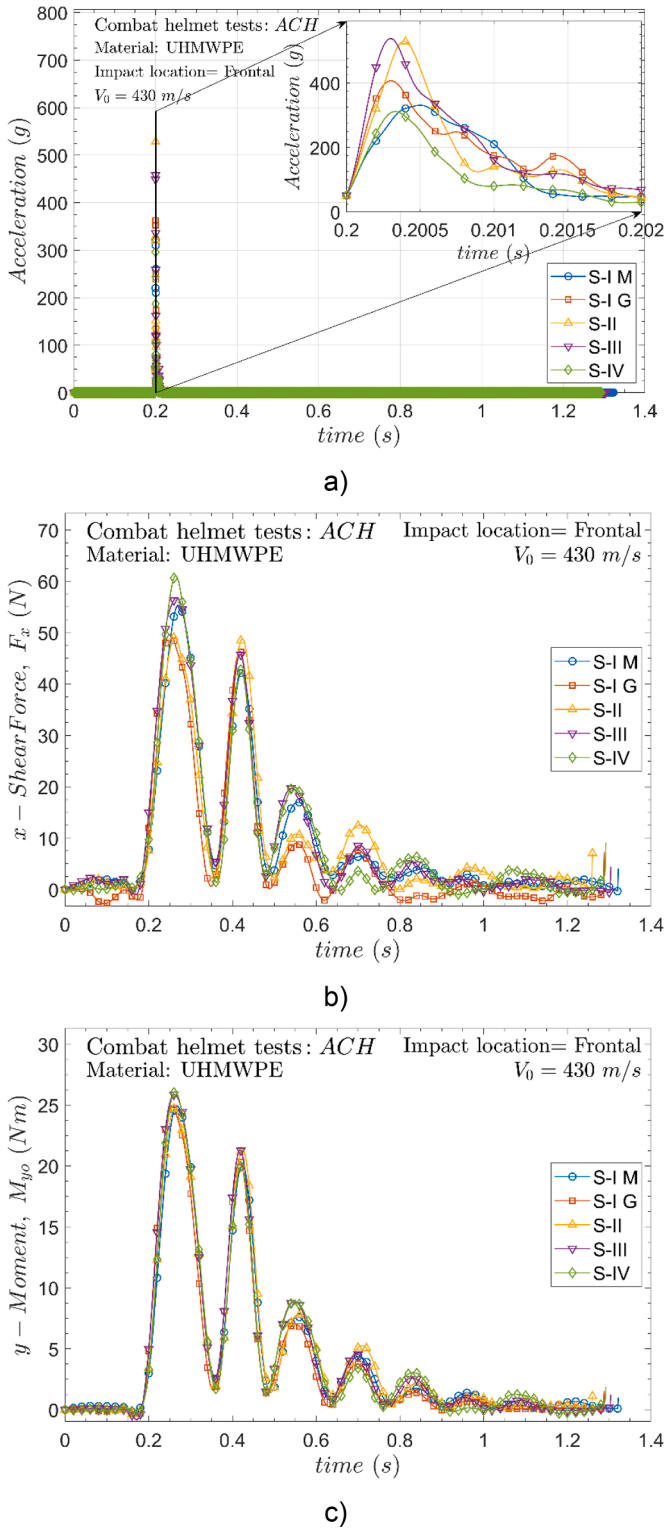

Fig. 8. a) Linear accelerations, b) x- shear forces, and c) y-moment temporal history.

2.5. Assessing injury

The analysis of personal protective equipment requires improvements in evaluating the protection from the biomechanical damage induced in the body. The Hybrid III dummy measures longitudinal accelerations at the head's center of mass and forces and momentum in the lower neck. Based on these parameters, different damage indicators for the brain and neck are described below.

2.5.1. Peak linear acceleration (PLA)

Maximum acceleration is the simplest indicator of TBI. Cranial bone failure and intracranial overpressure are related to the critical level of maximum PLA, as stated by NIJ 0106.01 regulation equal to *400 g*. This threshold value is associated with severe TBI according to the United States Federal Motor Vehicle Safety Standard (FMVSS) 571.218 for motorcycle helmets [41]. However, without considering the duration of the pulse, PLA may have a low correlation with TBI [51]. Therefore, a combination of acceleration level below the critical threshold of *400 g* and pulse duration of the acceleration can lead to severe head injury severity. The Wayne State Concussion Tolerance Curve (WSTC) was proposed [51,52] to relate the translational PLA to the duration of the acceleration pulse, Fig. 5. The zone under the curve implies the condition of having no head injuries.

2.5.2. HIC criterion

Head Injury Criteria (HIC) based on the WSTC is one of the most used injury assessment criteria in the automotive sector. Eq. (3) provides a maximum value integrating the acceleration *a(t)* in the range time (t_1, t_2). Critical HIC values are obtained from automotive tests. For example, a critical threshold of HIC = 1000, for an impact duration of 36 ms, was proposed by the United States National Highway Traffic Safety Administration (NHTSA) [41] or equal to *2400* established by the European Standard ECE R22/05 [54] for motorcycle helmets. However, this criterion is controversial for *0 – 5 ms* (representative of a ballistic impact) because HIC allows a head acceleration that produces significant intracranial pressures in the head, so HIC does not provide enough protection for a short duration [55].

$$HIC = \left\{ \left[\frac{1}{t_2 - t_1} \int_{t_1}^{t_2} a(t)dt \right]^{2.5} (t_2 - t_1) \right\}_{max} \tag{3}$$

For clarity in the analysis of the assessment of injury, the probability of damage severity can be obtained using the Abbreviated Injury Scale (AIS). AIS is related to the HIC and is calculated through the curves developed by Hayes et al. [56], as illustrated in Fig. 6. Table 2 shows the probability of different injury modes.

2.6. Neck injury criteria

The NHTSA established critical force and moment thresholds for the Hybrid III dummy neck ($F_x = 3100\ N, M_{yo} = 114\ Nm$) [57]. Recently, Yoganandan et al. [45] concluded critical threshold values for the lower neck of the Hybrid III -the lower neck refers to the vertebrae from C3/C5 to C7 (depending on the author/work)-. Nightingale et al. [58] developed experimental tests in males and fixed the mean bending tolerance of the lower cervical spine ($M_{y0} = 17.1\ Nm$). The values for female may be even lower due to the different configuration of the muscle-skeletal system of women around the neck.

Yoganandan et al. [45] developed a specific criterion for the lower neck, the LNI (Low Neck Injury) criterion, as a combination of shear force and the extension moment. LNI is a dimensionless scalar parameter defined in Eq. (4).

$$LNI = \frac{M_{yo}}{M_{crit}} + \frac{F_x}{F_{crit}} \tag{4}$$

where M_{crit}, and F_{crit} are critical constants, and their values are 117 *N·m* and 565 *N*, respectively, for the Hybrid III dummy [45].

The probability of neck injury is obtained with the maximum value of the LNI value. Yoganandan et al. [45] related the injury probability for the Hybrid III dummy through the curve in Fig. 7.

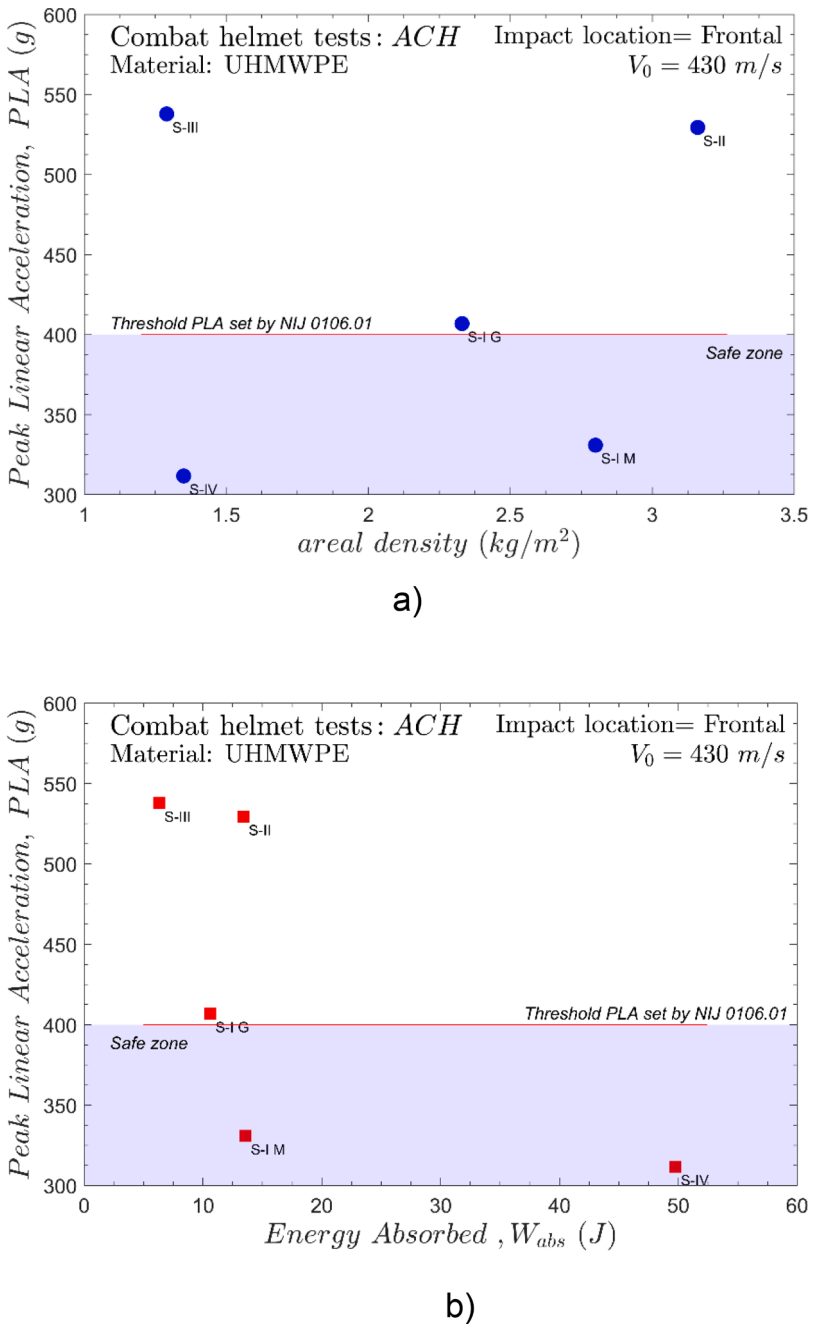

Fig. 9. Relation between Peak Linear Acceleration (PLA) and (a) areal density and (b) energy absorbed for the different pad systems.

3. Results

This section displays the direct results obtained from the accelerometers and neck load cell.

3.1. Linear acceleration time histories

The time evolution of the resultant acceleration for the different helmet pad configurations at *430 m/s* impact velocity is shown in Fig. 8a). The acceleration pulses are sinusoidal with defined resultant magnitudes and durations. The pulses consist of two distinct slopes: a rapid ascent to the maximum acceleration peak, followed by a gradual descent. In particular, the S-I G, S-II, and S-III cases exhibit a distinct slope. Differences in slope descent, as depicted by the curves, can be attributed to the damping properties of the foams.

The pulse shape is similar to the results observed under combat helmets in blunt impact conditions [48,59], but with lower impulse durations in this work, as expected. Maximum accelerations occur around 0.5 ms after an acceleration increase due to the impact starts to be registered. The maximum acceleration values were obtained from the pad system S-III, followed by the pad system S-II with *537 g* and *530 g*, respectively. The safest configurations are the S-IV and S-I M pad systems with *311* and *330 g*, respectively.

3.2. Forces and moments in the lower neck

Forces recorded in the impact direction (*x-axis*) and the moment on the *y-axis* are shown in Fig. 8b)-c). The curves recorded for the different pad systems are similar. Peak forces and moments occur at times after 0.1 s from the onset of impact. These data are consistent with Bass et al.

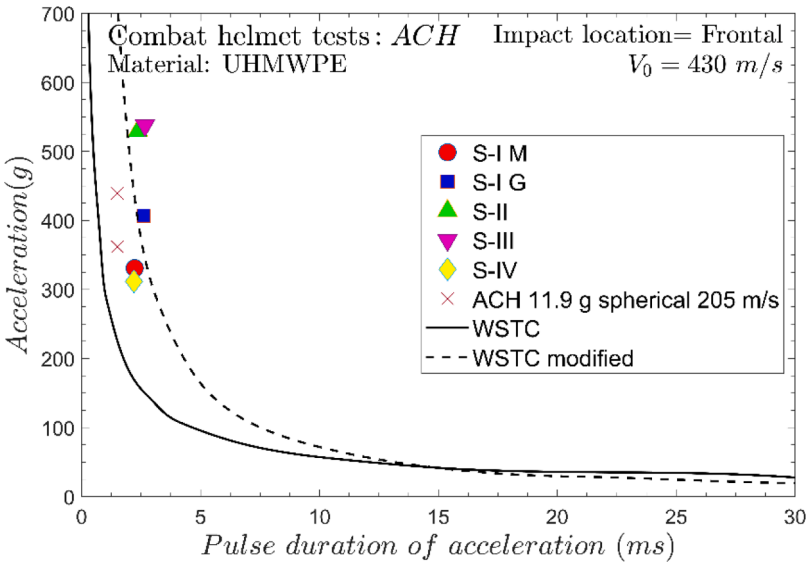

Fig. 10. Data compared to the Wayne State Tolerance Curve (WSTC) and modified Wayne State Tolerance Curve (modified WSTC) curves.

Table 3
Results of the Head Injury Criteria (HIC) and Abbreviated Injury Scale (AIS). Values that exceed the NHTSA threshold (HIC = 1000) are highlighted in gray.

Pad system	HIC	AIS 1 (%)	AIS 2 (%)	AIS 3 (%)	AIS 4 (%)	AIS 5 (%)	AIS 6 (%)
S-I M	884.94	98.98	81.14	41.85	17.95	1.06	0.02
S-I G	1009.46	99.73	89.36	53.58	24.57	2.22	0.06
S-II	1381.49	100.00	98.92	82.74	48.10	12.42	1.08
S-III	1608.12	100.00	99.83	92.75	62.72	26.90	4.18
S-IV	495.26	77.37	36.53	11.05	4.07	0.04	0.00

Table 4
Maximum force, moment, LNI, and neck injury probability (P) in the lower neck for each configuration.

	x-shear force (N)	y-moment (Nm)	LNI (-)	P (%)
S-I M	55.37	24.94	0.310	0.291
S-I G	49.57	24.85	0.299	0.270
S-II	49.14	24.72	0.298	0.267
S-III	56.79	25.86	0.321	0.317
S-IV	61.10	26.08	0.331	0.348

[60] since they demonstrated the highest values of cervical injury due to the forces and moments of a ballistic impact occurring for timescales greater than *0.05 s*.

4. Discussion

The impact of the 9 mm FMJ projectile onto the UHMWPE helmet, that is mounted on the Hybrid III dummy head, have demonstrated the influence of the pad configuration on longitudinal accelerations. This section discusses the results that have been translated to brain/neck injury indicators and the trauma of the postmortem combat helmet.

- Traumatic Brain Injury (TBI)

Peak linear acceleration (PLA) is commonly used as a criterion for TBI. The plot of PLA versus the areal density of the pad systems is shown in Fig. 9a. The increase in foam areal density does not seem to be a fully deterministic parameter. The S-I M ($t = 21\ mm$, $\rho_{areal} = 2.8\ kg/m^2$) shows similar results to the S-IV ($t = 21\ mm$, $\rho_{areal} = 1.35\ kg/m^2$).

Fig. 9b shows the relationship between PLA and the energy absorption capacity of the pad systems. The increase in the foam absorption capacity implies a decrease in the PLA. It is noteworthy to highlight how the S-II system has an energy absorption capacity (13.41 J) similar to the SI-M (13.58 J); however, the PLA value is higher ($PLA_{S-II} = 529.3\ g > 330.8\ g = PLA_{S-I\ M}$). This behavior may be due to the padding system architecture based on closed-cell foam, which collapsed earlier, as shown in Fig. 1b. This collapse mechanism can lead to higher g-accelerations during impact.

The energy absorption of S-I M and S-IV is significantly higher than the other configurations. The results show that only the S-I M and S-IV pad systems are in the safety zone since they are below the linear acceleration limit (*400 g*) set by NIJ 0106.01 [47] and Federal Motor Vehicle Safety Standard [41].

Comparing foams for the same material (S-I M and S-I G) demonstrates the importance of foam thickness. A similar conclusion was reported by Palomar et al [61]. They revealed a critical stand-off distance of 19 mm for a 59 cm circumference head at which cranial and brain injury occurred. However, our results show that the configuration and mechanical properties of the foams are also relevant for establishing this threshold stand-off distance. Therefore, neither thickness nor areal density are the unique parameters for designing the interior foam system of the combat helmet.

As commented previously, another approach to analyze TBI by accelerations is to consider the duration of the acceleration pulse. This criterion is known as the Wayne State Tolerance Curve (WSTC). Recently, Hoshizaki et al. [62] developed a WSTC revision with data from contact sports. Fig. 10 shows the results obtained in this work, other ballistic data from the literature [63], and the modified WSTC [62]. The represented results demonstrate that all configurations are over the original WSTC curve, which was not developed for phenomena with short acceleration pulse duration. However, the modified WSTC was developed by Hoshizaki et al. [62] with short acceleration pulse durations ($< 5\ ms$) since it was performed with data from falls resulting in "*persistent post-concussive syndrome*" (patients who had symptoms of concussion longer than a three-month period after the accident) and TBI falls [62]. Thus, most of the accelerations obtained in this work are below the modified WSTC curve. Originally, the tests conducted to perform the WSTC were performed with low-speed animal and skull impacts with durations longer than 5 ms and with collisions in football or combat sports involving durations up to 20 ms [62]. Consequently, Hoshizaki collected data from falls and pedestrian accidents to modify the original curve as described in Fig. 10.

The estimated HIC values from the accelerations measured in the

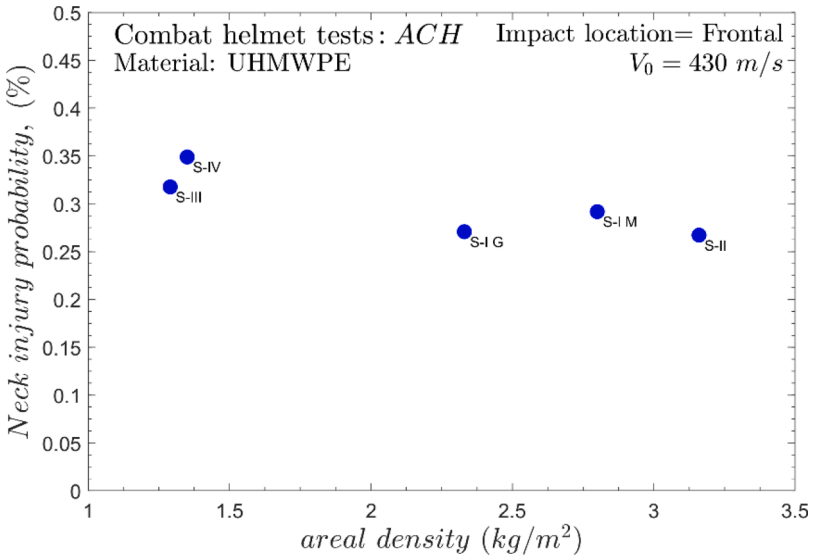

Fig. 11. Injury probability versus areal density.

Hybrid III dummy and the abbreviated injury scale (AIS) diagnostic metrics [56] are summarized in Table 3. The HIC values that exceed the NHTSA threshold (HIC = 1000) are found in the S-I G, S-II and S-III systems.

It is worth noting that despite the maximum acceleration being relatively similar in the S-I M and S-IV systems (as seen in Fig. 7a), there is a significant difference in HIC values, with ΔHIC≈390. This considerable difference in HIC values could be linked to the shape of the acceleration curves and the slope's decline after the peak acceleration is reached. The faster the drop of acceleration over time, the less HIC is obtained; therefore, more attenuation of the acceleration reaching the brain and more energy absorption capacity of the pads. Therefore, based on the HIC criterion, the S-I M and S-IV foam configurations are deemed the safest, aligning with the PLA criterion findings.

According to the AIS scale (shown previously in Table 2 of Section 2.5.2), our results show a high probability of level 1 and 2 injuries in all cases. However, the likelihood of $AIS \geq 3$ is low (<50%) for S-I M, S-I G, and S-IV. TBI associated with *AIS 3* is unconsciousness during *1 –6 h* and depressed fracture. *AIS 6* is related to the death of an individual and is practically non-existent in all cases. According to this analysis, the S-IV pad system is the safest option.

- Analysis of neck injury

The neck injury analysis is performed with the maximum values for the forces and moments of the curves presented in Fig. 8a–c. The maximum force values and the maximum moments are summarized in Table 4.

All values are below the Hybrid III tolerance levels established by the National Highway Traffic Safety Administration (NHTSA), $F_x = 3100\ N$ and $M_{yo} = 114\ Nm$ [41]. Also, our results are below the threshold values of forces and moments for the lower neck in the Hybrid III ($F_x = 565\ N$, $M_{yo} = 117\ Nm$) according to the work recently developed by Yoganandan et al. [45]. All the probabilities of neck injury obtained for the different configurations are below 1%. These results agree with those of Bass et al. [60], which indicated that the probabilities of neck injury for impact velocities between 400 and 460 m/s for a 9 mm FMJ projectile were less than 10%. We have used a combat helmet of different base material (UHMWPE) and four other pad systems so that we could find significant differences concerning the study of Bass et al. Furthermore, our study focuses on the lower neck due to the placement of our neck load cell, in contrast to Bass' work, which focused on the upper neck.

In addition, the configurations with the highest probability of neck injury correspond to those with the lowest areal density and weight, as shown in Fig. 11. This conclusion agrees with the scientific literature: "*increased helmet mass will tend to delay and decrease neck forces and may mitigate the potential for injury*" [35]. In our study, there is no significant difference in the total weight of the helmet shell assembly and the foam interior system. However, the helmet's weight should not be too high for the user's comfort. So, a compromise must be reached between safety and helmet weight.

- Postmortem analysis of the helmets

The permanent backface deformation of the specimen (PBFD) after impact is measured using the 3D scanner, Fig. 12a). This technique provides the displacement field at any point on the helmet's surface. All deflections are lower than 25.4 mm, the threshold value required by the DOT&E (Office of the Director, Operational Test and Evaluation) for helmet impacts by a 9 mm projectile for frontal or rear impacts [64]. The PBFD results also may indicate that skull rupture would not occur according to Rafaels et al. [14] since the impact velocity of our work (430 m/s) is below 500 m/ s, the threshold for a 20-year-old male wearing a UHMWPE helmet.

Fig. 12b) shows the relationship of PBFD with the areal density of the foam system. There is no clear correlation between PBFD and areal density. The pad system with the best PBFD performance is S-I-M (*15.61 mm*) versus S-IV (*21.27 mm*). The results reveal that the areal density is irrelevant since the lightest systems (S-III and S-IV) and the heaviest systems (S-II) have high deformation values. The energy absorption capacity does not seem to be a relevant parameter either. However, let's compare the S-I-M and S-II configurations, which have the same thickness, and their curves in Fig. 1. It is found that the S-I M pad, which presents higher deformation capacity, leads to a lower PBFD (*15.61 mm*). The other pad systems have reached their maximum energy-absorbing capacity. Future investigations using the finite element method can corroborate this claim more precisely.

For clarity, a summary table, Table 5, has been developed to show which brain injury criteria are met by foam systems. The thicker bi-component system (S-I M) and the S IV system, consisting of a sandwich configuration with a honeycomb panel core, are the safest for the studied brain and neck injury criteria.

This study allows manufacturers, designers, and researchers in combat helmets to have advanced knowledge of how the proposed configurations would perform in the face of other threats such as falls, explosions, or other munitions. The present study is carried out

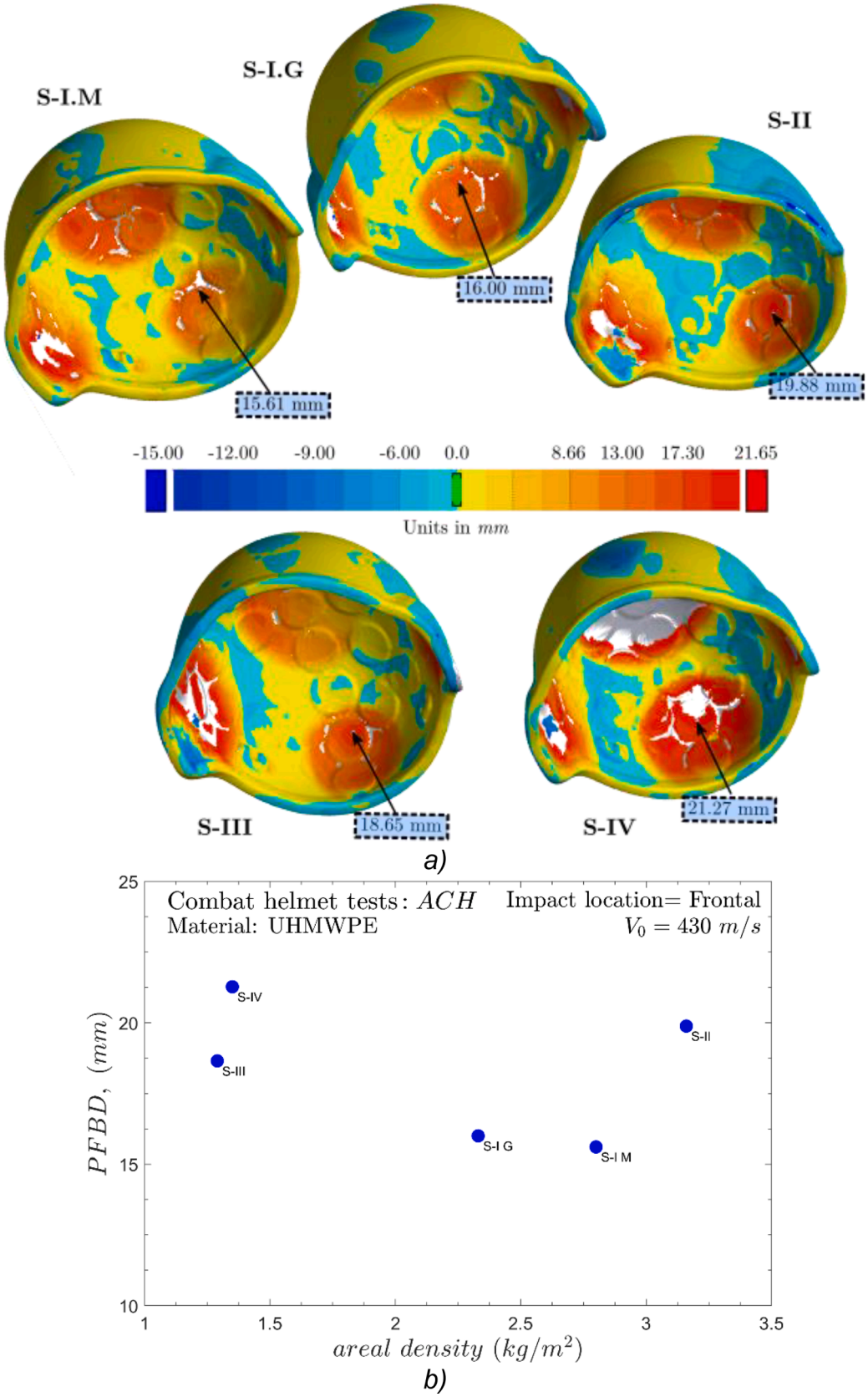

Fig. 12. a) Permanent backface deformation of the interior frontal side of the helmet using the 3D scanner b) Permanent backface deformation vs. areal density.

Table 5
Summary of foam systems evaluated using the injury criteria. The criteria that foam systems meet are highlighted in green, whereas those that they do not meet are highlighted in red.

Injury criteria / Pad system	PLA	Modified WSTC	HIC	NHTSA neck	LNI	PBFD
S-I M						
S-I G						
S-II						
S-III						
S-IV						

PLA: Peak Linear Acceleration; HIC: Head Injury Criteria; NHTSA neck Hybrid III tolerance levels; LNI: Lower Neck Injury, PFBD: Permanent backface deformation.

according to NIJ 0106.01, i.e., perpendicular impacts at 5 m with an impact velocity of 425 m/s. For 9 mm FMJ firearms, this velocity could hardly be exceeded; however, the results should be simulated. For other impact conditions, such as oblique impacts or lower velocities, the authors believe there will be no difference in the conclusions obtained from the present work. The present study lays the groundwork for future studies and new experimental campaigns and allows us to develop valid numerical models with experimental results.

5. Conclusions

This study conducted an experimental analysis of the performance of four pad systems for combat helmets to mitigate brain and neck injuries under ballistic impact using 9 mm FMJ. The Hybrid III dummy allowed recording longitudinal accelerations in the brain and forces and moments at the lower neck. These variables were translated into injury parameters for assessing damage risk for the user.

The experimental results obtained in this paper are synthesized as follows:

- A strong influence of the foam is revealed in the mitigation of brain injury. The difference in the peak linear acceleration between the foams can be more than *200 g* among the pad systems analyzed in our study.
- The areal density of the foams was not found to be a key parameter in comparison to the energy absorption capacity of the foam.
- Permanent backface deformation is another parameter considered for the design of combat helmets. The results suggest that there was no risk of skull fracture below the deformation threshold for the cases considered.
- Foams with greater thickness and high SEA values (J/g) perform better in minimizing brain and neck injury.
- According to the acceleration criteria, the foam configured with the honeycomb core panel (S-IV) was the most effective in mitigating brain accelerations.
- The different criteria (PLA, WSTC, HIC, PBFD) showed similar results, although the HIC criterion is considered the most appropriate. Furthermore, the thickness of the pad for the same foam has a notable influence.
- The results showed probabilities of neck injuries lower than 1% in all cases.
- The results were in accordance with the scientific literature, as the higher the weight of the helmet-foam system set, the lower the probability of neck injury.

Having performed the analysis and obtained the main conclusions of the work, the study's main limitations are the biofidelity of the metallic dummy headform, of which only its kinematic responses can be obtained. A new trend is to use digital twins of human heads made by 3D printing and ballistic gelatin as brain simulant. Using numerical FEM models would allow for obtaining more damage-related parameters such as brain stresses, strains, pressures, and deformations. Another area for improvement in the present study is the inability to know each foam's compression level once the combat helmet is placed on the head surrogate. However, this study provides a basis for future research using FEM tools, and it can be of great help when designing combat helmets to mitigate brain and neck injury.

CRediT authorship contribution statement

M. Rodriguez-Millan: Conceptualization, Investigation, Validation, Writing – original draft, Visualization, Funding acquisition. **I. Rubio:** Writing – original draft, Investigation, Validation, Writing – review & editing. **F.J. Burpo:** Writing – original draft, Investigation, Writing – review & editing, Visualization. **A. Olmedo:** Conceptualization, Resources. **J.A. Loya:** Conceptualization, Resources, Investigation, Writing – original draft, Writing – review & editing, Funding acquisition, Supervision. **K.K. Parker:** Writing – original draft, Investigation, Writing – review & editing, Visualization. **M.H Miguélez:** Conceptualization, Resources, Funding acquisition, Supervision, Project administration.

Declaration of Competing Interest

The authors declare that they have no known competing financial interests or personal relationships that could have appeared to influence the work reported in this paper.

Data availability

Data will be made available on request.

Acknowledgments

The authors acknowledge the Ministry of Economy and Competitiveness of Spain and the FEDER program under Projects DPI2017-88166-R and PID2020-118946RB-I00 for the financial support of the work. M. Rodriguez-Millan acknowledges the Spanish Ministry of Universities, the National Program for the Promotion of Talent, and its Employability in Research and Development and Innovation (R&D&I), National Mobility Subprogram of the National Plan for Scientific and Technical Research and Innovation 2021–2023, for the professor's mobility program (PRX21/00329). It has to thank the funding for APC: Universidad Carlos III de Madrid (Read and Publish Agreement CRUE-CSIC 2023).

References

[1] Hemphill MA, Dauth S, Yu CJ, Dabiri BE, Parker KK. Traumatic brain injury and the neuronal microenvironment: a potential role for neuropathological mechanotransduction. Neuron 2015;85:1177–92. https://doi.org/10.1016/j.neuron.2015.02.041.
[2] Ortega Zufiría JM, Prieto NL, Cuba BC, Degenhardt MT, Núñez PP, López Serrano MR, López Raigada AB. Mild head injury. Surg Neurol Int 2018;9:S16–28. https://doi.org/10.4103/sni.sni_371_17.

[3] Reger MA, Brenner LA, Du Pont A. Traumatic brain injury and veteran mortality after the War in Afghanistan. JAMA Netw Open 2022;5:2021–3. https://doi.org/10.1001/jamanetworkopen.2021.48158.

[4] Agtarap S, Campbell-Sills L, Thomas ML, Kessler RC, Ursano RJ, Stein MB. Postconcussive, posttraumatic stress and depressive symptoms in recently deployed U.S. Army soldiers with traumatic brain injury. Psychol Assess 2019;31:1340–56. https://doi.org/10.1037/pas0000756.

[5] Kong LZ, Zhang RL, Hu SH, Lai JB. Military traumatic brain injury: a challenge straddling neurology and psychiatry. Mil Med Res 2022;9:2. https://doi.org/10.1186/s40779-021-00363-y.

[6] Tham CY, Tan VBC, Lee HP. Ballistic impact of a KEVLAR® helmet: experiment and simulations. Int J Impact Eng 2008;35:304–18. https://doi.org/10.1016/j.ijimpeng.2007.03.008.

[7] Tan LBin, Tse KM, Lee HP, Tan VBC, Lim SP. Performance of an advanced combat helmet with different interior cushioning systems in ballistic impact: experiments and finite element simulations. Int J Impact Eng 2012;50:99–112. https://doi.org/10.1016/j.ijimpeng.2012.06.003.

[8] Rubio I, Rodríguez-Millán M, Marco M, Olmedo A, Loya JA. Ballistic performance of aramid composite combat helmet for protection against small projectiles. Compos Struct 2019;226. https://doi.org/10.1016/j.compstruct.2019.111153.

[9] Rubio I, Díaz-Álvarez A, Bernier R, Rusinek A, Loya JA, Miguelez MH, Rodríguez-Millán M. Postmortem analysis using different sensors and technologies on aramid composites samples after ballistic impact. Sensors (Switzerland) 2020;20. https://doi.org/10.3390/s20102853.

[10] Rodríguez-Millán M, Ito T, Loya JA, Olmedo A, Miguélez MH. Development of numerical model for ballistic resistance evaluation of combat helmet and experimental validation. Mater Des 2016;110:391–403. https://doi.org/10.1016/j.matdes.2016.08.015.

[11] Palta E, Fang H, Weggel DC. Finite element analysis of the advanced combat helmet under various ballistic impacts. Int J Impact Eng 2018;112:125–43. https://doi.org/10.1016/j.ijimpeng.2017.10.010.

[12] Li YQ, Li XG, Gao XL. Modeling of advanced combat helmet under ballistic impact. J Appl Mech Trans ASME 2015;82. https://doi.org/10.1115/1.4031095.

[13] Freitas CJ, Mathis JT, Scott N, Bigger RP, MacKiewicz J. Dynamic response due to behind helmet blunt trauma measured with a human head surrogate. Int J Med Sci 2014;11:409–25. https://doi.org/10.7150/ijms.8079.

[14] Rafaels KA, Cutcliffe HC, Salzar RS, Davis M, Boggess B, Bush B, Harris R, Rountree MS, Sanderson E, Campman S, et al. Injuries of the head from backface deformation of ballistic protective helmets under ballistic impact. J Forensic Sci 2015;60:219–25. https://doi.org/10.1111/1556-4029.12570.

[15] Aare M, Kleiven S. Evaluation of head response to ballistic helmet impacts using the finite element method. Int J Impact Eng 2007;34(3):596–608. https://doi.org/10.1016/j.ijimpeng.2005.08.001.

[16] Halldin P, Lanner D, Coomber R, Kleiven S. Evaluation of blunt impact protection in a military helmet designed to offer blunt & ballistic impact protection. In: 1st International conference on helmet performance and design; 2013.

[17] Salimi Jazi M, Rezaei A, Karami G, Azarmi F, Ziejewski M. A computational study of influence of helmet padding materials on the human brain under ballistic impacts. Comput Methods Biomech Biomed Engin 2014;17(12):1368–82. https://doi.org/10.1080/10255842.2012.748755.

[18] Yang J, Dai J. Simulation-based assessment of rear effect to ballistic helmet impact. Comput Aided Des Appl 2010;7(1):59–73. https://doi.org/10.3722/cadaps.2010.59-73.

[19] Li XG, Gao XL, Kleiven S. Behind helmet blunt trauma induced by ballistic impact: a computational model. Int J Impact Eng 2016;91:56–67. https://doi.org/10.1016/j.ijimpeng.2015.12.010.

[20] Chang L, Guo Y, Huang X, Xia Y, Cai Z. Experimental study on the protective performance of bulletproof plate and padding materials under ballistic impact. Mater Des 2021;207:109841. https://doi.org/10.1016/j.matdes.2021.109841.

[21] Pintar FA, Philippens MMGM, Zhang JY, Yoganandan N. Methodology to determine skull bone and brain responses from ballistic helmet-to-head contact loading using experiments and finite element analysis. Med Eng Phys 2013;35:1682–7. https://doi.org/10.1016/j.medengphy.2013.04.015.

[22] Miranda-Vicario A, Bravo PM, Coghe F. Experimental study of the deformation of a ballistic helmet impacted with pistol ammunition. Compos Struct 2018;203:233–41. https://doi.org/10.1016/j.compstruct.2018.07.012.

[23] Begonia M, Humm J, Shah A, Pintar FA, Yoganandan N. Influence of ATD versus PMHS reference sensor inputs on computational brain response in frontal impacts to advanced combat helmet (ACH). Traffic Inj Prev 2018;19:S159–61. https://doi.org/10.1080/15389588.2018.1532214.

[24] Tse KM, Tan LB, Yang B, Tan VBC, Lee HP. Effect of helmet liner systems and impact directions on severity of head injuries sustained in ballistic impacts: a finite element (FE) study. Med Biol Eng Comput 2017;55:641–62. https://doi.org/10.1007/s11517-016-1536-3.

[25] Cai Z, Huang X, Xia Y, Li G, Fan Z. Study on behind helmet blunt trauma caused by high-speed bullet. Appl Bionics Biomech 2020. https://doi.org/10.1155/2020/2348064.

[26] Zhang L, Yang KH, King AI. Comparison of brain responses between frontal and lateral impacts by finite element modeling. J Neurotrauma 2001;18(1):21–30. https://doi.org/10.1089/089771501750055749.

[27] Bottlang M, DiGiacomo G, Tsai S, Madey S. Effect of helmet design on impact performance of industrial safety helmets. Heliyon 2022;8(8):e09962. https://doi.org/10.1016/j.heliyon.2022.e09962.

[28] Darling T, Muthuswamy J, Rajan SD. Finite element modeling of human brain response to football helmet impacts. Comput Methods Biomech Biomed Engin 2016;19(13):1432–42. https://doi.org/10.1080/10255842.2016.1149574.

[29] Matsui Y, Oikawa S, Hosokawa N. Effectiveness of wearing a bicycle helmet for impacts against the front of a vehicle and the road surface. Traffic Inj Prev 2018;19(7):773–7. https://doi.org/10.1080/15389588.2018.1498089.

[30] Karton C, Rousseau P, Vassilyadi M, Hoshizaki TB. The evaluation of speed skating helmet performance through peak linear and rotational accelerations. Br J Sports Med 2014;48(1):46–50. https://doi.org/10.1136/bjsports-2012-091583.

[31] O'Sullivan DM, Fife GP, Pieter W, Shin I. Safety performance evaluation of taekwondo headgear. Br J Sports Med 2013;47(7):447–51. https://doi.org/10.1136/bjsports-2012-091416.

[32] Post A, Karton C, Blaine Hoshizaki T, Gilchrist MD, Bailes J. Evaluation of the protective capacity of baseball helmets for concussive impacts. Comput Methods Biomech Biomed Engin 2016;19(4):366–75. https://doi.org/10.1080/10255842.2015.1029921.

[33] Rodriguez-Millan M, Rubio I, Burpo FJ, Tse KM, Olmedo A, Loya JA, Miguélez MH. Experimental and numerical analyses of ballistic resistance evaluation of combat helmet using hybrid III headform. Int J Impact Eng 2023. https://doi.org/10.1016/j.ijimpeng.2023.104653. In-press. 104653.

[34] National Research Council (U.S.). Committee on Testing Armor Materials for Use by the U.S. Army.; National Research Council (U.S.). Board on Army Science and Technology.; National Research Council (U.S.). Committee on National Statistics.; National Research Council (U.S.). Division on Engineering and Physical Sciences.; National Research Council (U.S.). Division of Behavioral and Social Sciences and Education. Testing of body armor materials : phase III. National Academies Press; 2012. ISBN 9780309255998.

[35] National Research Council (U.S.). Committee on review of test protocols used by the DoD to test combat helmets Review of department of defense test protocols for combat helmets; ISBN 9780309298667.

[36] Mertz HJ, Patrick LM. Strength and response of the human neck. SAE Trans 1971:2903–28.

[37] Mertz HJ, Hodgson VR, Thomas LM, Nyquist GW. An assessment of compressive neck loads under injury-producing conditions. Phys Sportsmed 1978;6(11):95–106.

[38] Nyquist, G.W., Begman, P.C., King, A.I., & Mertz, H.J. Correlation of field injuries and GM hybrid III dummy responses for lap-shoulder belt restraint. 1980.

[39] Prasad P, Daniel RP. A biomechanical analysis of head, neck, and torso injuries to child surrogates due to sudden torso acceleration. SAE Trans 1984:784–99.

[40] Kleinberger M, Sun E, Eppinger R, Kuppa S, Saul R. Development of improved injury criteria for the assessment of advanced automotive restraint systems. NHTSA Docket 2018;4405(9):12–7.

[41] Administration, N.H.T.S. Motor vehicle safety; 2008; Vol. 372, p. 527;.

[42] Yoganandan N, Kumaresan S, Pintar FA. Geometric and mechanical properties of human cervical spine ligaments. J Biomech Eng 2000;122:623–9. https://doi.org/10.1115/1.1322034.

[43] Yoganandan N, Banerjee A, Hsu FC, Bass CR, Voo L, Pintar FA, Gayzik FS. Deriving injury risk curves using survival analysis from biomechanical experiments. J Biomech 2016;49(14):3260–7. https://doi.org/10.1016/j.jbiomech.2016.08.002.

[44] Yoganandan N, Pintar FA, Banerjee A. Load-based lower neck injury criteria for females from rear impact from cadaver experiments. Ann Biomed Eng 2017;45:1194–203. https://doi.org/10.1007/s10439-016-1773-5.

[45] Yoganandan N, Humm J, Greenhalgh P, Somers J. Lower neck injury criteria for THOR and hybrid III dummies in rear impact. Traffic Inj Prev 2020;0:1–3. https://doi.org/10.1080/15389588.2020.1829925.

[46] Begonia MT, Pintar FA, Yoganandan N. Comparison of NOCSAE head kinematics using the hybrid III and EuroSID-2 necks. J Biomech 2018;80:37–44. https://doi.org/10.1016/j.jbiomech.2018.08.018.

[47] Standard, N.I. of J. (NIJ) NILECJ-STD-0106.00: ballistic helmets; 1981;.

[48] Begonia M, Rooks T, Pintar FA, Yoganandan N. Development of a methodology for simulating complex head impacts with the advanced combat helmet. Mil Med 2019;184:237–44. https://doi.org/10.1093/milmed/usy282.

[49] Rodríguez-Millán M, Tan LB, Tse KM, Lee HP, Miguélez MH. Effect of full helmet systems on human head responses under blast loading. Jmade 2016;117:58–71. https://doi.org/10.1016/j.matdes.2016.12.081.

[50] Engineers, S. of A. SAE recommended practice: instrumentation for impact test-part 1-electronic instrumentation. Society of Automotive Engineers, Warrendale, PA, SAE J211/1 Dec03.; 2003;.

[51] Gadd CW. Impact acceleration stress. Washington, D.C.: National Academies Press; 1962. ISBN 978-0-309-34021-2.

[52] Lissner HR, Lebow M, Evans FG. Experimental studies on the relation between acceleration and intracranial pressure changes in man. Surg Gynecol Obstet 1960;111:329–38.

[53] Gurdjian ES, Roberts VL, Thomas LM. Tolerance curves of acceleration and intracranial pressure and protective index in experimental head injury. J Trauma Inj Infect Crit Care 1966;6:600–4. https://doi.org/10.1097/00005373-196609000-00005.

[54] (UNECE), U.N.E.C. for E. ECE 22 05, Uniform provision concerning the approval of protective helmets and their visors for driver and passengers of motor cycles and mopeds; 2002; Vol. Regulation, pp. 1–11;.

[55] Álvarez-Caldas C, Quesada A, Román JLS, Olmeda E. Head injury criterion: the best way to evaluate head damage? Int J Veh Des 2007;45:411–25. https://doi.org/10.1504/IJVD.2007.014913.

[56] Hayes WC, Erickson MS, Power ED. Forensic injury biomechanics. Annu Rev Biomed Eng 2007;9:55–86. https://doi.org/10.1146/annurev.bioeng.9.060906.151946.

[57] Eppinger, R.; Sun, E.; Bandak, F.; Haffner, M.; Khaewpong, N.; Maltese, M.; Kuppa, S.; Nguyen, T.; Takhounts, E.; Tannous, R.; et al. Development of improved injury criteria for the assessment of advanced automotive restraint systems - II; 1999;.
[58] Nightingale RW, Carol Chancey V, Ottaviano D, Luck JF, Tran L, Prange M, Myers BS. Flexion and extension structural properties and strengths for male cervical spine segments. J Biomech 2007;40:535–42. https://doi.org/10.1016/j.jbiomech.2006.02.015.
[59] Moure-Guardiola C, Rubio I, Antona-Makoshi J, Olmedo Á, Loya JA, Rodríguez-Millán M. Evaluation of combat helmet behavior under blunt impact. Appl Sci 2020:1–22. https://doi.org/10.3390/app10238470.
[60] Bass CR, Donnellan L, Salzar R, Lucas S, Folk B, Davis M, Rafaels K, Planchak C, Meyerhoff K, Ziemba A, et al. A new neck injury criterion in combined vertical/frontal crashes with head supported mass. In: Int. Res. Counc. Biomech. Impact - 2006 Int. IRCOBI Conf. Biomech. Impact, Proc; 2006. p. 75–91.
[61] Palomar M, Lozano-Mínguez E, Rodríguez-Millán M, Miguélez MH, Giner E. Relevant factors in the design of composite ballistic helmets. Compos Struct 2018;201:49–61. https://doi.org/10.1016/j.compstruct.2018.05.076.
[62] Hoshizaki TB, Post A, Kendall M, Cournoyer J, Rousseau P, Gilchrist MD, Brien S, Cusimano M, Marshall S. The development of a threshold curve for the understanding of concussion in sport. Trauma (United Kingdom) 2017;19:196–206. https://doi.org/10.1177/1460408616676503.
[63] Lei T, Xie L, Tu W, Chen Y, Tan Y. Development of a finite element model for blast injuries to the pig mandible and a preliminary biomechanical analysis. J Trauma Acute Care Surg 2012;73:902–7. https://doi.org/10.1097/TA.0b013e3182515cb1.
[64] DOT&E Standard for lot acceptance ballistic testing of hard body armor. 2010. Arlington, Va.